2024-01-5070 Published 18 Jul 2024

Analysis of Motor Cooling Lines of Electric Buses with 1D Models and Verification with Experiments

Azim Turan, Emrah Yaki, Çağrı Emre Birgül, and Hakan Kaya Anadolu ISUZU

Citation: Turan, A., Yaki, E., Birgül, Ç.E., and Kaya, H., "Analysis of Motor Cooling Lines of Electric Buses with 1D Models and Verification with Experiments," SAE Technical Paper 2024-01-5070, 2024, doi:10.4271/2024-01-5070.

Received: 08 Feb 2024 Revised: 24 Apr 2024 Accepted: 13 Jun 2024

Abstract

Improving the overall thermal management strategy in electric vehicles can directly or indirectly improve battery efficiency and vehicle range. The aim of this study is to simulate and improve the performance of motor cooling lines developed for an electric bus using 1D computational fluid dynamics models. In the study, simulation studies were carried out for the 12-m EV Citivolt vehicle of Anadolu Isuzu. Design parameters such as placement of flow lines and component selection were decided thanks to 1D models developed. The design obtained at the end of the study was supported by tests and experimental studies. As a result, it was seen that the components in the line correctly detected the flow rate and pressure losses with a maximum error rate of 8% and an average error rate of 4.8%. Additionally, the components on the line were added to the model via their own characteristic dp-Q curves. In this way, it has been seen that these components, which contain complex flow lines, can be represented with unique dp-Q curves.

Keywords

Motor cooling, Electric bus, Test & validation, 1D system simulation

Introduction

Electrification of the transportation sector is one of the most important steps for sustainable and clean transportation. According to 2023 data, the transportation sector plays an important role in carbon emissions with a rate of nearly 20% [1]. According to studies, the ratio of electric buses in total electric passenger transportation is expected to increase to 80% by 2040 [2]. By developing optimized vehicles in three areas such as cost, lifespan, and driving range, electric buses can provide advantages over internal combustion engine buses. Developing highly efficient and integrated engine cooling systems can have a positive impact on these three topics.

However, the development of suitable cooling systems requires additional auxiliary components or subsystems, resulting in an increase in the weight of the total system and, more importantly, in energy consumption. To overcome this trade-off problem and minimize energy consumption, the operation strategy of cooling units must be optimized. The aim of this study was to develop accurate and easy simulations to assess the motor cooling system performances.

Electrical components have specific resistances due to the electrical elements they contain, resulting in heat energy generation. The heat energy thus produced is conveyed to the cooling fluid through cooling channels within the component. In cases where the flow rate and technical specifications of the cooling fluid passing through the cooling channels are inadequate, the thermal load generated by the component may expose the component to high temperatures. Since thermal and physical properties of the coolant play a vital role in determining the system efficiency, the cooling fluid should possess certain properties, such as high thermal capacity, low kinematic viscosity, and high corrosion resistance [3]. As a demonstration of impact of the fluid properties on heat transfer, Reference [4] showed that adding nanoparticles to the coolant fluid can significantly improve the cooling efficiency.

According to [5] hybrid heat rejection strategies could save up to 33% of the power consumption while the operating condition is secured. Dual-phase heat transfer devices such as thermosiphons and heat tubes are passive cooling systems that enable heat transfer. Highly efficient passive cooling systems can be developed by expanding the heat transfer surface area and/or integrating materials with high thermal conductivity. In addition, conventional liquid cooling systems are more preferred in urban public transportation applications such as buses that require high heat transfer. Reference [6] explored the integration of advanced control algorithms to the cooling system of a mid-size truck for military applications, with the aim of achieving temperature tracking for vehicle safety and energy efficiency. They found that liquid cooling systems using electromechanical actuators instead of mechanical parts showed high efficiency. Reference [7] compared electric and hydraulic fans in cooling systems for different climatic conditions and revealed the benefits of electric fans.

The development of cooling systems for hybrid electric vehicles and the need for an optimal strategy to minimize energy consumption were discussed [8]. They introduced an approach for finding the optimal control strategy of the electric auxiliaries over a defined driving cycle and proposed a mixed integer linear program to solve the optimization problem.

Reference [9], on the other hand, examined the flows inside the radiator and showed that heat transfer and radiator performance can be increased with designs that create low pressure loss. In his large-scale experimental study, Reference [10] examined the pressure losses created by laminar, transitional, and turbulent flows in circular cross-sectional tubes and the effects of these losses on heat transfer. It is found that the limits for pressure drop and heat transfer in different flow regimes are the same and that a direct relationship exists between pressure drop and heat transfer even in the transitional flow regime.

In the laminar flow regime, the relationship between pressure drop and heat transfer can be expressed as a function of the Grashof number (due to free convection effects), and in the other three flow regimes as a function of the Reynolds number.

These results lead us to the conclusion that the engine cooling line in the vehicle should be modeled to create low pressure losses.

Mathematical Modeling

In a flow cycle in which the fluid flows without phase change, changes in channel cross-sections and flow direction cause some of the total energy of the fluid to be irreversibly converted into heat energy.

For single-phase, steady-state, and incompressible flows, the pressure loss can be calculated by the following equation:

$$\Delta p = f \times \frac{L}{d} \times \frac{\rho \times v^2}{2} \qquad \text{Eq. (1)}$$

An extra pressure loss term due to the gravitational acceleration did not include this equation since the elevation change for a piping system in a vehicle is relatively small. While modeling the flow lines in the study, the pressure loss equation was transformed into the following equation by expressing the fluid velocity in terms of the cross-sectional area of the pipe and the constant flow rate throughout the system:

$$\Delta p = 8f \times \frac{L}{d^5} \times \frac{\rho \times Q^2}{2\pi^2} \qquad \text{Eq. (2)}$$

With reference from [11], the following formulas were used for turbulent and laminar flows, which is the friction coefficient f:

$$f_{laminar} = \frac{64}{Re} \qquad \text{Eq. (3)}$$

$$f_{turbulent} = \frac{0.25}{\left[\log_{10}\left(\frac{5.74}{Re^{0.9}} + \frac{K/d}{3.7}\right)\right]^2} \qquad \text{Eq. (4)}$$

where the Reynolds number Re is calculated as:

$$Re = \frac{vd}{\nu} \qquad \text{Eq. (5)}$$

The effect of elbows in the flow line on pressure loss was modeled with the coefficient C_a. The following transformations were used:

$$\Delta p = f \times C_a \times \frac{L}{d} \times \frac{\rho \times v^2}{2} \qquad \text{Eq. (6)}$$

For flow branches and conferences along the line, pressure losses were calculated using the following formula:

$$\Delta p_{i,j} = C_{a(i,j)} \frac{\rho v^2}{2} C_{Re} \qquad \text{Eq. (7)}$$

Here, the notations i and j represent the connecting or separating flow branches (Figure 1).

FIGURE 1 Connecting and separating branches in flow systems.

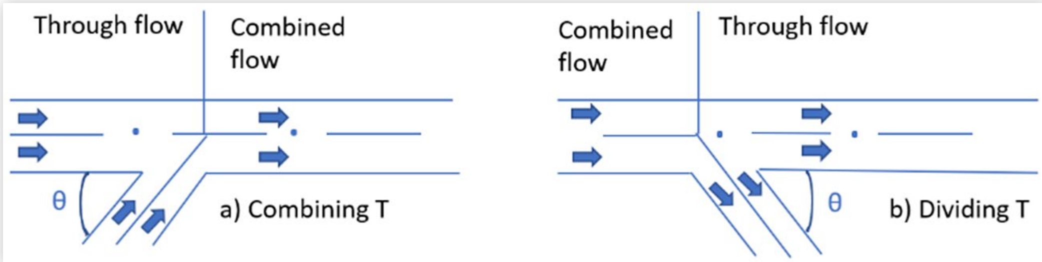

Test Procedures and Experimental Studies

Vehicle tests were carried out at the Anadolu ISUZU Test Center. A 12-m EV Citivolt vehicle of Anadolu Isuzu was selected due to its common usage in urban transportation as a 12 m low-floor vehicle. The representative view of the coolant system was given in Figure 2. Thermocouple was used to instantly examine the coolant temperature. In this way, temperature changes during flow measurements were controlled, and it was aimed to prevent flow rate changes due to viscosity changes that would occur due to high temperature/cold effect. The DC–DC converter is an electromechanical device or circuitry used to convert a DC voltage from one level to another based on circuit requirements. It is an essential component in electric vehicles, where several electronic circuits are operating at different voltage levels.

Thermocouple and flow meters were placed in the areas indicated in Figure 3. The selected pressure points are the inlet and outlet points of each component. In this way, the pressure drops that will occur in the systems were calculated and the maximum pressure criteria of the components were examined. Flow meters are placed inside each component to measure the fluid flow rate passing through the components.

When selecting the coolant for a bus, it's essential to consider corrosion and freezing during winter. To avoid freezing, it's crucial to include antifreeze, like glycol, in the coolant mixture. BASF Glicentin G48 coolant with a mixture of 50% glycol and 50% water recommended by the electric motor and inverter supplier was used (Table 1).

Test Measuring Point

The dp-Q curves of the circulation pump at 2100 RPM, 3000 RPM, 3200 RPM, 3500 RPM, and 3900 RPM were used. To make a one-to-one comparison, KULI simulations and flow tests were performed only in these specific periods. During the flow test, the coolant temperature varies between 23°C and 28°C. Ambient temperature is 20°C. At the beginning of the test, the temperature of the cooling liquid was 23°C. While the pump provides energy to the cooling liquid, a portion of this energy is converted into heat, causing the temperature of the cooling liquid to increase. As a result, at the end of the test, the temperature of the cooling liquid had reached 28°C. Flow meters are connected to the system in series.

FIGURE 2 Motor cooling system's actual layout.

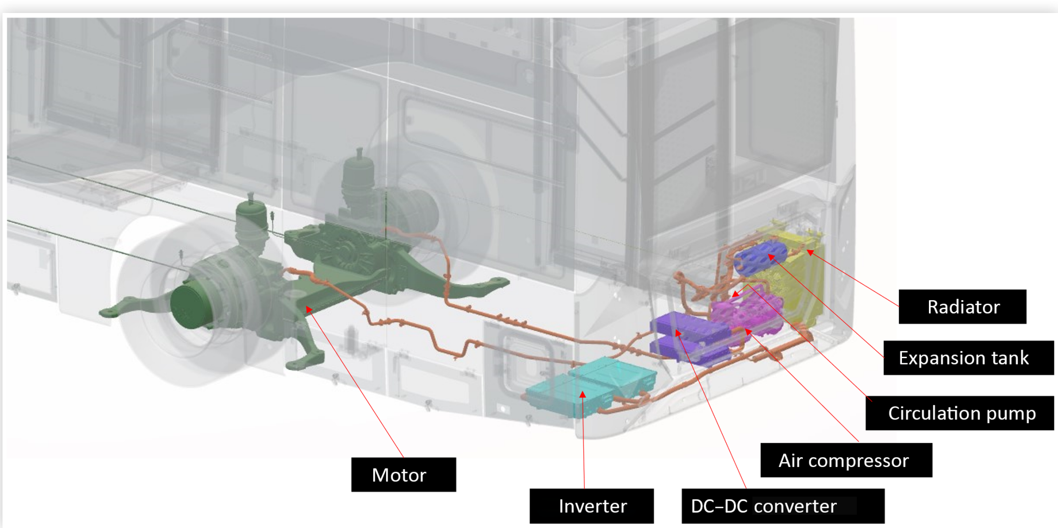

FIGURE 3 Bus cooling system layout and measurement locations. Green and orange points show flowmeter locations and thermocouple location respectively.

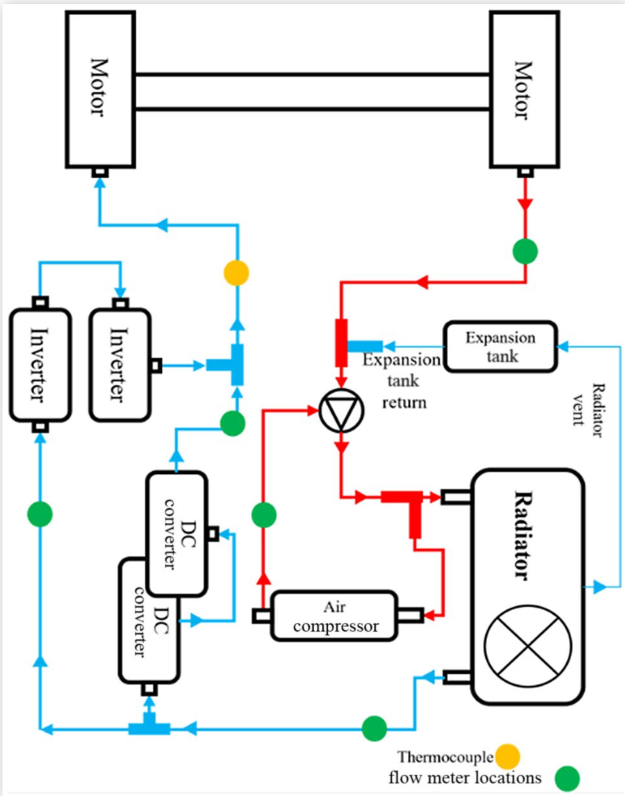

TABLE 1 Properties of coolant.

Density at 20°C	1.072–1.074 g/cm³
Kinematic viscosity at 20°C	4.1 mm²/s

TABLE 2 Instrumentation.

Flowmeter SM6020: IFM-SM6020 model magnetic–inductive flow meter was used to measure flow values	
Cold Junction Thermocouple Box A thermocouple was used to measure the temperature of the cooling liquid. The thermocouple was connected to SoMat Cold Junction Thermocouple Box, Type K–16	
SoMat eDAQ Base Processor: The data received with the cold junction thermocouple box and pressure meters was interpreted and recorded with the data collection center	

The instruments and their applications were given at Tables 2 and 3, respectively. Mass flows were measured at outlet sections of every component. Flow meters are connected to the system in series.

For the coolant temperature measurement, the thermocouple was placed on the motor side. The temperature information was transmitted to the cold junction thermocouple box via the green-colored cable, where it was identified. The circulation pump speed was changed via CAN Bus communication and the flow rate values were read after the system was in mode.

The minimum and maximum allowable flow rates for the components are listed at Table 4.

1D Modeling Details

Mathematical characterization of complex thermodynamic systems can be achieved through one-dimensional (1D) calculations. KULI (a comprehensive system-level simulation software) energy management software used in this study was developed by STEYR engineering. KULI is a 1D software for design and simulation in vehicle thermal management systems. It supports balancing performance between different components and between components and the system.

Figure 4 shows the model image taken from the KULI interface. Flow rates were extracted at the inlet port of each component. The dp-Q curves of the components within the cooling system, through which the cooling fluid passes, have been obtained from component suppliers. Due to commercial concerns, the dp-Q curves of these components cannot be shared.

Flow direction can be followed by looking at component inlets and outlets. The flow line distributes to the radiator and air compressor components at the pump outlet, and to the DC converter and inverter components at the radiator outlet. As a result, the line flow is divided.

To keep the flow rates to the components at an adequate level, it is necessary to consider both the pressure loss in the components and the pressure drops that occur at elbows, separations, and junctions in the line. In the process of modeling the flow line, each turn, elbow, separation, and junction point in the pipelines was added to the KULI model as a separate component. In

TABLE 3 Flow rate sensor locations.

Air compressor	
Motor	
DC–DC converter	
Inverter	
Radiator	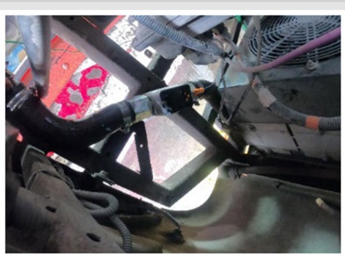

TABLE 4 Components' minimum and maximum allowable flow rates. Provided by the suppliers.

	Air compressor	DC–DC converter	Motor	Inverter
Min. flow rate (L/min)	10	6	—	—
Max. flow rate (L/min)	14	20	25	25

FIGURE 4 KULI model view. Green and red boxes represent tube inlets and outlets, respectively.

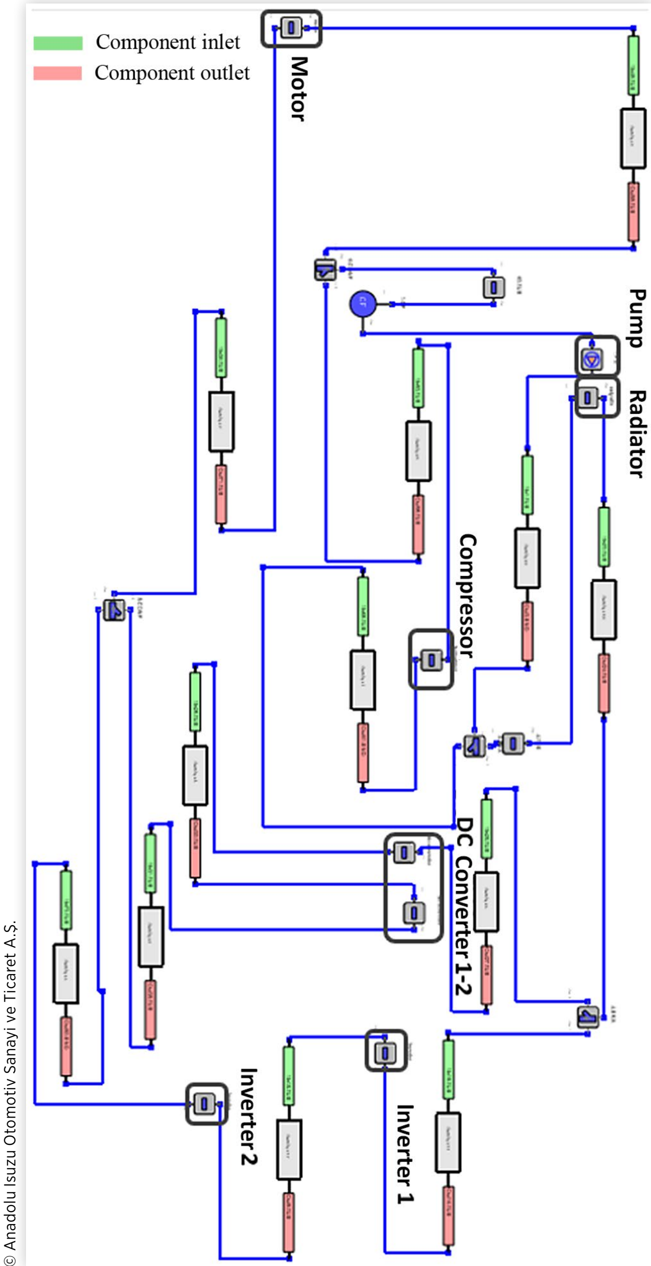

addition, the characteristic dp-Q curves of the pump, motor, radiator, air compressor, dc–dc converter, and inverter components are used for the relevant component. These curves were provided by the components' producers. In this way, the pressure losses occurring on the line could be transferred to the model to a large extent.

The pressure drop equations introduced in the mathematical modeling section were applied to each component in the model by calculating the mean pressures [12]:

$$p = \frac{p_{in} + p_{out}}{2} \qquad \text{Eq. (5)}$$

where p_{in} and p_{out} are the inlet and outlet pressures on the component, respectively. The pipe diameter d of the flow system varies between 5 mm (compressor inlet) and 38 mm (radiator inlet). The minimum and maximum *Re* numbers are 2800 and 16,000, which concludes that the flow is in a turbulence flow regime.

Results

In simulations, computations were performed using the Intel® Xeon® E5-2640 processors with a single processor core, and the computations averaged 2.12 s. In general, simulation results showed good agreement with the experimental data. It is observed that simulation results are much closer to the test at higher pump speeds.

Table 5 shows the components' flow rates in L/min units. Results were compared at different pump speeds. While the percentage of the mean difference is close to 10% at 2100 RPM, it reduced to 4% at 3900 RPM. It is also observed that overall the highest and the lowest deviations were observed at the air compressor and DC converter components, respectively. Highlighted red cells indicate that the coolant flow rates are outside the limits. According to the test data, the circulation pump for the cooling system should operate within the range of 3000 RPM and 3500 RPM. However, based on the KULI results, the circulation pump for the cooling system should operate within the range of 3000 RPM and 3200 RPM.

Comparing Table 4 with Table 5, it can be concluded that at the test and KULI results, air compressor failed at 2100 RPM due to violation of minimum flow rate limit, which is 10 L/min. Both the air compressor and the motor failed at 3900 RPM pump speed because of its maximum flow rate limit, which is 14 L/min for the air compressor and 25 L/min for motor. At 3500 RPM, the air compressor failed due to the violation of maximum flow rate according to KULI results, while the test gave more optimistic results.

Table 6 shows the percent of difference between KULI simulations and test results. Individual component-wise comparison between the experimental results and the numerical results were given in Figure 5. The maximum deviation occurred as 16% at the inverter component at 2100 RPM pump speed. Also, minimum deviation was observed as less than 1% at the DC–DC converter component at 3900 RPM pump speed.

The pressure drops of components for different pump speeds that were taken from simulation results were given at Table 7.

Summary/Conclusions

In this study, the virtually designed vehicle cooling system of the 12-m EV Citivolt vehicle of Anadolu Isuzu was modeled in the KULI program and the analysis results were verified through tests. The outcome of this study was to gain an ability to use 1D simulations to assess and improve the motor cooling line performance. KULI analysis

TABLE 5 KULI and test results of the flow rates of the components according to different pump speeds.

		Pump speed (RPM)				
		2100	3000	3200	3500	3900
Air compressor flow rate (L/min)	KULI	8.5	12.5	13.5	14.6	16.6
	TEST	7.4	11.2	12	13.3	15.3
Motor flow rate (L/min)	KULI	14.5	21	23	24	28
	TEST	12.8	19.6	21.2	23.5	27
Radiator flow rate (L/min)	KULI	14.5	21	23	24	28
	TEST	12.8	19.6	21.2	23.5	27
DC–DC converter flow rate (L/min)	KULI	6.5	10	11	11.8	13.45
	TEST	6.12	9.5	10.28	11.4	13.4
Inverter flow rate (L/min)	KULI	7.8	11	12	13	14.5
	TEST	6.7	10.2	11	12.1	13.96

Red cells indicate the violation of components' flow rate limits.

TABLE 6 Deviations of results between KULI simulations and tests.

	Pump speed (RPM)				
	2100 (%)	3000 (%)	3200 (%)	3500 (%)	3900 (%)
Air compressor	15	12	13	10	8
Motor	13	7	8	2	4
Radiator	13	7	8	2	4
DC–DC converter	6	5	7	4	0
Inverter	16	8	9	7	4

FIGURE 5 Flow rates' results of components for different pumps speeds.

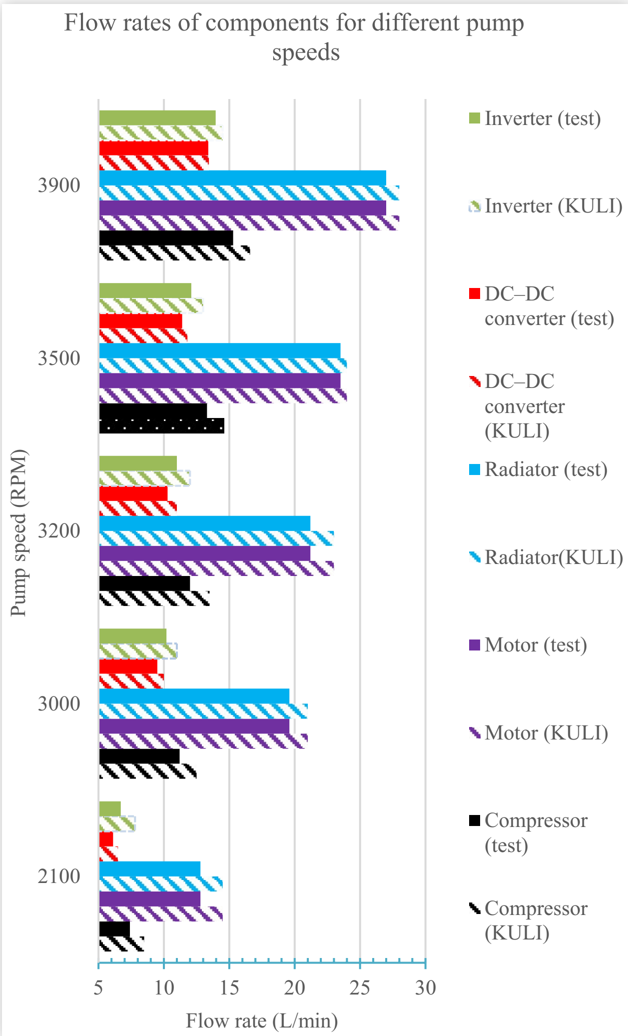

was run for specific circulation pump speeds, considering the technical specifications of the components in the cooling system. After the analysis method and solution method are verified, it is planned to use this model in other tools in the future, so it is important to verify this model and solution method with experimental tests. Table 5 showed that the pump RPM should be between 3000 RPM and 3500 RPM.

The margin of error between coolant simulations' experimental testing decreases at high circulation pump speeds. Height differences in the lines, sagging in the pipes, ignoring the in-pipe roughness values of the connection parts, and convergence of the intermediate values in the dp-Q curves cause a margin of error.

Also, the thermal effects are ignored in the simulations. System performance is calculated based on flow rates only. With this approach, model complexity is reduced, and solution time is shortened. However, changes in fluid properties resulting from temperature changes and the effects of these changes could not be detected. It is thought that some of the errors in Table 6 arise from this.

With a cooling system algorithm to be prepared for the vehicle, the circulation pump speed can be changed in line with the cooling demand of the air compressor. At the same time, the circulation pump will operate at maximum when another component requires maximum cooling. In this case, a resistance will be added to the air compressor line to prevent the flow rate of coolant passing through the compressor from being exceeded.

As a conclusion, by using the validated KULI models, the flow rates in parallel lines can be adjusted for the desired values, then the cooling line can be physically updated. In new vehicle designs or layout updates, optimum results can be achieved quickly and reliably with 1D models instead of setting up a physical model and performing flow tests for each iteration.

Definitions/Abbreviations

C_a - Loss coefficient
C_{Re} - Reynolds correction coefficient
d - Tube inner diameter (m)
f - Darcy's friction factor
L - Tube length (m)
p - Pressure (Pa)
Q - Flow rate (m³/s)
Re - Reynolds number
v - Fluid velocity (m/s)
ρ - Fluid density (kg/m³)

TABLE 7 Pressure drops of each component for different pump speeds obtained from simulations.

	Pump speed (RPM)				
	2100	3000	3200	3500	3900
Air compressor (kPa)	14.14	31.3	36.3	41.8	54
Motor (kPa)	14.78	32.87	38.2	44	57
Radiator (kPa)	0.16	0.31	0.36	0.41	0.54
DC–DC converter (kPa)	0.58	1.15	1.27	1.39	1.7
Inverter (kPa)	2.95	6.52	7.55	8.67	11

References

1. Pal, P., Gopal, P.R.C., and Ramkumar, M., "Impact of Transportation on Climate Change: An Ecological Modernization Theoretical Perspective," *Transport Policy* 130 (2023): 167-183.
2. Manzolli, J.A., Trovao, J.P., and Antunes, C.H., "A Review of Electric Bus Vehicles Research Topics – Methods and Trends," *Renewable and Sustainable Energy Reviews* 159 (2022): 112211.
3. Raj, J.A.P.S., Asirvatham, L.G., Angeline, A.A., Manova, S. et al., "Thermal Management Strategies and Power Ratings of Electric Vehicle Motors," *Renewable and Sustainable Energy Reviews* 189 (2024): 113874.
4. Bouselsal, M., Mebarek-Oudina, F., Biswas, N., and Ismail, A.A.I., "Heat Transfer Enhancement Using Al_2O_3-MWCNT Hybrid-Nanofluid inside a Tube/Shell Heat Exchanger with Different Tube Shapes," *Micromachines* 14 (2023): 1072.
5. Shoai Naini, S., Huang, J., Miller, R., Wagner, J. et al., "An Innovative Electric Motor Cooling System for Hybrid Vehicles - Model and Test," SAE Technical Paper 2019-01-1076 (2019), doi:https://doi.org/10.4271/2019-01-1076.
6. Tao, X., Zhou, K., Ivanco, A., Wagner, J. et al., "A Hybrid Electric Vehicle Thermal Management System - Nonlinear Controller Design," SAE Technical Paper 2015-01-1710 (2015), doi:https://doi.org/10.4271/2015-01-1710.
7. Fernandes, R., "Efficient Volvo Bus Cooling System, Using Electrical Fans: A Comparison between Hydraulic and Electrical Fans," 2014, accessed 12 January 2024, https://urn.kb.se/resolve?urn=urn:nbn:se:kth:diva-155901.
8. Kitanoski, F. and Hofer, A., "A Contribution to Energy Optimal Thermal Management for Vehicles," *IFAC Proceedings Volumes* 43, no. 7 (2010): 87-92.
9. Głogoza, A., Janicka, A., Włostowski, R., and Zawiślak, M., "Numerical Optimalization of the Electric Bus Radiator in Terms of Noise Emissions and Energy Consumption," 2021.
10. Everts, M. and Meyer, J.P., "Relationship between Pressure Drop and Heat Transfer of Developing and Fully Developed Flow in Smooth Horizontal Circular Tubes in the Laminar, Transitional, Quasi-Turbulent and Turbulent Flow Regimes," *International Journal of Heat and Mass Transfer* 117 (2018): 1231-1250.
11. Miller, D., *Internal Flow Systems, BHRA* (Cranfield, UK: The Fluid Engineering Centre, 1990)
12. KULI, "KULI Documentation," 2022, accessed January 12, 2024, https://KULI.magna.com/company.

ISSN 0148-7191